

## Spin-orbit splitting in crystalline and compositionally disordered semiconductors

D. J. Chadi

*Xerox Palo Alto Research Center, Palo Alto, California 94304*

(Received 9 March 1977)

The electronic structures of C, Si, Ge,  $\alpha$ -Sn, GaP, GaAs, GaSb, InP, InAs, InSb, and ZnSe are studied using a tight-binding approach which includes spin-orbit interactions. The spin-orbit splittings  $\Delta_0$  and  $\Delta_1$  are related to atomic spin-orbit splittings and optical gaps. The variation of  $\Delta_0$  as a function of chemical composition is studied for a number of alloy systems. It is shown that the nonlinear dependence of  $\Delta_0$  on alloy composition is a disorder-induced effect. The bowing parameter is calculated in terms of tight-binding parameters and band gaps.

### I. INTRODUCTION

The spin-orbit (SO) splittings  $\Delta_0$  and  $\Delta_1$  of the valence bands at the  $\Gamma$  and  $L$  points of the Brillouin zone show large departures from a linear dependence on alloy composition in a number of alloy systems.<sup>1-6</sup> For example,<sup>1</sup> InAs<sub>0.5</sub>Sb<sub>0.5</sub> has a so splitting  $\Delta_0 \approx 0.3$  eV, which is nearly a factor of 2 smaller than that expected from a linear extrapolation of  $\Delta_0$  from InAs to InSb. Empirical rules which are quite successful in accounting for the nonlinear variation of  $\Delta_0$  with composition have been previously presented.<sup>7,8</sup> In this paper we use the tight-binding (TB) method<sup>9,10</sup> to study the SO splitting of valence bands in crystalline and compositionally disordered semiconductors. The TB model used provides a description of electronic states in terms of short-range interactions of electrons centered on nearest-neighbor atoms. The short-range nature of the interactions makes the TB method very useful in studying compositionally disordered alloys. The type of nearest-neighbor interactions used and their effect on electronic states are discussed in Sec. II. Tight-binding parameters for some diamond and zinc-blende crystals are also given in Sec. II. The relation of  $\Delta_0$  and  $\Delta_1$  to atomic SO splittings and optical gaps in crystalline systems is derived in Sec. III. The results provide the corrections to the well-known<sup>11,12</sup>  $\frac{2}{3}$  relation between  $\Delta_0$  and  $\Delta_1$ . The variation of  $\Delta_0$  with alloy composition is studied using several different models in Sec. IV. We find that the virtual-crystal approximation is inadequate in describing the experimental data since it leads to a linear variation of  $\Delta_0$  with alloying. A different model which avoids the averaging of TB parameters involved in the virtual-crystal approximation but leaves the system periodic is to assume a chalcopyrite structure for an intermediate alloy  $A_{0.5}B_{0.5}C$ . We find that the chalcopyrite model also predicts a nearly linear behavior of the SO splitting with alloying, as discussed in more detail in Sec.

IV. These calculations indicate that the nonlinear variation of  $\Delta_0$  is a disorder-induced effect. The major effect of compositional disorder is the mixing of  $s$  states into the  $p$  states at the top of the valence band.<sup>7</sup> The bowing parameter is related in Sec. IV to the difference in the  $s$ - $p$  interaction parameters of the alloy constituents. It is shown that TB parameters obtained by fitting the band structure to optical<sup>13</sup> and photoemission<sup>14,15</sup> data provide a satisfactory explanation for the observed nonlinear behavior of  $\Delta_0$  in substitutional alloy systems.

### II. TIGHT-BINDING MODEL AND PARAMETERS

The TB model we use is of the Slater-Koster<sup>9,10</sup> type. For diamond and zinc-blende crystals the Bloch functions are constructed of  $s$  and  $p$  orbitals (Wannier functions) centered on each atom in the crystal. It is assumed that the only nonzero Hamiltonian matrix elements are those between orbitals on the same or adjacent atoms. This results in a relatively good description of the valence bands throughout the Brillouin zone.<sup>10</sup> The conduction bands at  $\vec{k}=0$  are fitted to experimental<sup>13</sup> optical data. A good description of the conduction bands particularly along the (100) direction requires the inclusion of  $d$  orbitals<sup>16</sup>; this would, however, make the empirical TB method impractical to use.

Denoting the  $s$  and  $p$  orbitals on the two atoms of the primitive cell by  $|s_i\rangle$ ,  $|x_i\rangle$ ,  $|y_i\rangle$ , and  $|z_i\rangle$ , with

$$i = 1 = \text{anion}, \quad i = 2 = \text{cation}, \quad (1)$$

the interactions between orbitals with same spin are (as in Ref. 10)

$$E_{s_i} = \langle s_i | H | s_i \rangle, \quad i = 1, 2, \quad (2)$$

$$E_{p_i} = \langle x_i | H | x_i \rangle, \quad i = 1, 2, \quad (3)$$

$$V_{ss} = 4 \langle s_1 | H | s_2 \rangle, \quad (4)$$

$$V_{xx} = 4 \langle x_1 | H | x_2 \rangle, \quad (5)$$

$$V_{xy} = 4\langle x_1 | H | y_2 \rangle, \quad (6)$$

$$V_{s_1 p_2} = 4\langle s_1 | H | x_2 \rangle, \quad (7)$$

$$V_{s_2 p_1} = -4\langle s_2 | H | x_1 \rangle. \quad (8)$$

The interactions  $V_{s_1 p_2}$  and  $V_{s_2 p_1}$  are equal in group-IV crystals. The factor of 4 in Eqs. (4) to (8) is used for convenience; these parameters are related to the interaction of an orbital on one atom with four equivalent nearest-neighbor orbitals on adjacent atoms. In the notation of  $\sigma$  and  $\pi$  interactions, the parameters are  $V_{ss\sigma} = \frac{1}{4}(V_{ss})$ ,  $V_{pp\sigma} = \frac{1}{4}(V_{xx} + 2V_{xy})$ ,  $V_{pp\pi} = \frac{1}{4}(V_{xx} - V_{xy})$ ,  $V_{s_1 p_2 \sigma} = (\sqrt{3}/4)V_{s_1 p_2}$ , and  $V_{s_2 p_1 \sigma} = (\sqrt{3}/4)V_{s_2 p_1}$ .

The spin-orbit component of the Hamiltonian,

$$H_{SO} = (\hbar/4m^2c^2)[\nabla V \times \vec{p}] \cdot \vec{\sigma}, \quad (9)$$

where  $V$  is the total (crystal) and  $\vec{\sigma}$  represents the Pauli spin matrices, couples  $p$  orbitals on the same atom, e.g.,

$$\langle x_i \uparrow | H_{SO} | z_i \downarrow \rangle = \lambda_i, \quad i = 1, 2, \quad (10)$$

where  $\uparrow, \downarrow$  denote spin states, and with

$$\lambda_1 = \frac{1}{3}\Delta_a, \quad \lambda_2 = \frac{1}{3}\Delta_c, \quad (11)$$

where  $\Delta_a$  and  $\Delta_c$  are the "renormalized" atomic SO splitting of the anion and cation  $p$  states. A renormalization of atomic SO splittings is necessary to obtain the correct SO splitting of the valence bands in a crystal.<sup>17-22</sup> The normalization factor is large and is about 1.5 in Ge.<sup>21</sup> This is the ratio of the SO splitting  $\Delta_0 \approx 0.29$  eV at  $\Gamma$  to the free-atom SO splitting of about 0.2 eV. A normalization factor of about the same value works well in describing the SO splittings of other diamond and zinc-blende crystals.<sup>21,22</sup> Renormalized atomic SO splittings for atoms in solid environments obtained from several sources<sup>21,23,24</sup> are shown in Table I. There are two effects contributing to the renormalization. The first is basically a volume effect<sup>20</sup> arising from the tendency of Wannier functions to be localized in a volume larger than that of a Wigner-Seitz cell. The second effect<sup>18,19</sup> arises from the fact that the states near the top of the valence bands which originate from atomic  $p$  levels are not

TABLE I. Renormalized spin-orbit splittings of valence  $p$  states.

	Al	Si	P	S
	0.024	0.044	0.067	0.074
Zn	Ga	Ge	As	Se
0.074	0.174	0.29	0.421	0.48
Cd	In	Sn	Sb	Te
0.227	0.392	0.80	0.973	1.10

completely  $p$ -like in character but have a large admixture of  $d$  (and higher angular momentum) character.<sup>13</sup>

Tight-binding parameters for some diamond and zinc-blende semiconductors are shown in Tables II and III. The energies of the  $s$  and  $p$  states are relative to the top of the valence band at  $\Gamma$ . The resulting energy bands at the  $\Gamma$ ,  $X$ , and  $L$  points of the Brillouin zone are shown in Tables IV and V. The bands have been fitted to photoemission,<sup>14,15</sup> optical,<sup>13</sup> and the pseudopotential results of Ref. 13.

The determination of TB parameters is relatively simple in group-IV crystals. In our notation the energy gap between the  $\Gamma_1$  conduction and valence bands is equal<sup>10</sup> to  $2V_{ss}$ ; the energy gap  $E'_0$  (Fig. 1) is equal to  $2V_{xx}$ ; knowing  $V_{ss}$  and  $V_{xx}$ , the energy gap  $E_0$  at  $\Gamma$  (Fig. 1) determines  $E_p - E_s$ ; the lowest doubly degenerate valence bands at  $X$  determine  $V_{sp}$ , and the higher two bands at  $X$  determine  $V_{xy}$ .<sup>10</sup> The width of the top two valence bands, when only nearest-neighbor interactions are used, is equal to the energy difference between the  $\Gamma$  and  $X$  points of the Brillouin zone and is given by  $4|V_{pp\pi}| = |V_{xy} - V_{xx}|$ . As shown previously,<sup>10</sup> this width is increased by about 1 eV by second-nearest-neighbor interactions. To have the correct average density of states, we have, therefore, determined  $V_{xy}$  by taking for  $X$  the average of the experimentally determined energies (relative to the top of the band) of the  $X_4$  and  $\Sigma_{\min}$  points of the Brillouin zone.

TABLE II. Tight-binding parameters for group-IV crystals. In the column on the right-hand side the energy difference between  $s$  and  $p$  states obtained in the tight-binding method is compared to calculated (Ref. 23) atomic values (in parentheses). The zero of energy is at the top of the valence band.

	$E_s$	$E_p$	$V_{ss}$	$V_{xx}$	$V_{xy}$	$V_{sp}$	$E_p - E_s$
C	-2.99	3.00	-21.20	3.00	13.00	13.89	5.99(7.39)
Si	-4.20	1.70	-8.30	1.715	5.40	6.37	5.90(6.58)
Ge	-5.85	1.50	-6.75	1.60	5.40	5.33	7.35(7.13)
$\alpha$ -Sn	-5.86	1.06	-5.44	1.33	4.85	4.25	6.92(5.74)

TABLE III. Tight-binding parameters for some zinc-blende crystals. The zero of energy is at the top of the valence band.

	$E_{p_1}$	$E_{p_2}$	$E_{p_1}-E_{s_1}$	$E_{p_2}-E_{s_2}$	$V_{ss}$	$V_{xx}$	$V_{xy}$	$V_{s_1p_2}$	$V_{s_2p_1}$
GaP	1.28	3.82	8.88	6.54	-7.66	2.26	6.20	5.33	5.84
GaAs	1.16	3.35	9.37	6.54	-6.76	2.11	5.96	4.75	5.48
GaSb	0.68	2.63	7.52	6.54	-6.06	1.64	4.32	5.55	4.76
InP	1.12	3.82	8.88	5.80	-5.59	2.12	4.90	3.81	5.25
InAs	1.03	3.35	10.54	5.80	-5.25	2.02	4.84	3.06	5.33
InSb	0.76	2.57	8.98	5.80	-5.43	1.71	4.46	3.93	4.76
ZnSe	0.96	6.06	13.13	6.19	-6.76	2.61	5.61	2.47	5.99

Similar considerations were used to obtain the parameters of zinc-blende semiconductors. Table III reveals a generally consistent trend for the variation of the TB parameters from one zinc-blende crystal to another. For these semiconductors we find that anion and cation  $p$  states (similarly for  $s$  states) are always closer in energy as compared to their free-atom limit.<sup>25</sup> This is reasonable and is caused primarily by the charge transfer from the cation to the anion. We also find that in all crystals (except for C and Si) the  $s$ - $p$  energy separation ( $E_p - E_s$ ) is always larger than its free-atom value.

### III. SPIN-ORBIT SPLITTING: CRYSTALS

Within the TB model described in Sec. II, explicit expressions for the SO splitting  $\Delta_0$  and  $\Delta_1$  at the  $\Gamma$  and  $L$  points of the Brillouin zone can be derived. For example, the energies of the  $\Gamma_8$  and  $\Gamma_7$  valence states are given by

$$E(\Gamma_8) = \frac{1}{2} (E_{p_1} + E_{p_2} + \lambda_1 + \lambda_2) - \frac{1}{2} [(E_{p_1} - E_{p_2} + \lambda_1 - \lambda_2)^2 + 4V_{xx}^2]^{1/2}, \quad (12)$$

$$E(\Gamma_7) = \frac{1}{2} (E_{p_1} + E_{p_2}) - (\lambda_1 + \lambda_2) - \frac{1}{2} [(E_{p_1} - E_{p_2} - 2\lambda_1 + 2\lambda_2)^2 + 4V_{xx}^2]^{1/2}, \quad (13)$$

where the relation of the  $\lambda_i$  to renormalized atomic SO splitting  $\Delta_i$  is given by Eq. (11). For group-IV crystals where  $E_{p_1} = E_{p_2}$  and  $\lambda_1 = \lambda_2$ , Eqs. (12) and (13) show that  $\Delta_0$  is equal to the renormalized SO splitting given in Table I. For zinc-blende semiconductors, since the inequality  $|\lambda_1 - \lambda_2| \ll |E_{p_1} - E_{p_2}|$  is usually very well satisfied, we can obtain a simple expression for  $\Delta_0$  by expanding the square roots in Eqs. (12) and (13). The energy difference  $E'_0$  (Fig. 1) is given by twice the value of the square-root term in Eq. (12). Using this we obtain

$$\Delta_0 \approx \frac{1}{2} (\Delta_a + \Delta_c) + \frac{1}{2} (\Delta_a - \Delta_c) (E_{p_2} - E_{p_1}) E'_0. \quad (14)$$

Since  $(E_{p_2} - E_{p_1}) > 0$  [see Eq. (1)], the second term

in Eq. (14) has the same sign as  $(\Delta_a - \Delta_c)$ . The values of  $\Delta_0$  obtained from the parameters given in Tables II and III are shown in Table VI and compared to experimental values. Equation (14) is similar in form to the empirical formula<sup>23</sup>

$$\Delta_0 = \frac{1}{2} (\Delta_a + \Delta_c) + \frac{1}{2} (\Delta_a - \Delta_c) f_i, \quad (15)$$

where  $f_i$  is the Phillips<sup>26</sup>-Van Vechten<sup>27</sup> ionicity parameter.

The SO splitting  $\Delta_1$  at  $L$  can also be related to the TB parameters. For the  $L_{4,5}$  and  $L_6$  valence bands we find

$$E(L_{4,5}) = \frac{1}{2} (E_{p_1} + E_{p_2} + \lambda_1 + \lambda_2) - \frac{1}{2} [(E_{p_1} - E_{p_2} + \lambda_1 - \lambda_2)^2 + (V_{xx} + V_{xy})^2]^{1/2} \quad (16)$$

and to an excellent approximation

TABLE IV. Energy levels of group-IV crystals at  $\Gamma$ ,  $X$ , and  $L$  points of the Brillouin zone obtained from the tight-binding method.

Point	Level	C	Si	Ge	$\alpha$ -Sn
$\Gamma$	$\Gamma_{6v}$	-24.19	-12.50	-12.60	-11.30
	$\Gamma_{7v}$	0.00	-0.045	-0.29	-0.80
	$\Gamma_{8v}$	0.00	0.00	0.00	0.00
	$\Gamma_{6c}$	18.21	4.10	0.90	-0.42
	$\Gamma_{7c}$	6.00	3.38	2.91	1.86
	$\Gamma_{8c}$	6.00	3.43	3.20	2.66
$X$	$X_{5v}$	-14.20	-8.27	-8.65	-7.88
	$X_{5b}$	-10.00	-3.70	-3.90	-3.80
	$X_{5c}$	14.21	5.77	4.30	3.07
$L$	$L_{6v}$	-18.04	-10.20	-10.50	-9.50
	$L_{6v}$	-14.20	-7.14	-7.41	-6.82
	$L_{6v}$	-10.00	-1.87	-2.10	-2.31
	$L_{4,5v}$	-10.00	-1.84	-1.90	-1.76
	$L_{6c}$	14.21	4.24	1.84	0.53
	$L_{6c}$	16.00	5.24	4.91	3.91
	$L_{4,5c}$	16.00	5.27	5.10	4.42

$$E(L_{\theta}) = \frac{1}{2}(E_{p_1} + E_{p_2} - \lambda_1 - \lambda_2) - \frac{1}{2}[(E_{p_1} - E_{p_2} - \lambda_1 + \lambda_2)^2 + (V_{xx} + V_{yy})^2]^{1/2}. \quad (17)$$

For group-IV crystals these equations give

$$\Delta_1 = \frac{2}{3} \Delta_0. \quad (18)$$

For zinc-blende crystals the expression for the SO splitting  $\Delta_1 = E(L_{4,5}) - E(L_{\theta})$  obtained from Eqs. (16) and (17) is well approximated by

$$\Delta_1 = \frac{1}{3}(\Delta_a + \Delta_c) + \frac{1}{3}(\Delta_a - \Delta_c)(E_{p_1} - E_{p_2})/E_L, \quad (19)$$

where  $E_L$  is the energy gap between the  $L_{4,5}$  valence and  $L_{4,5}$  conduction states. The above expression for  $\Delta_1$  is similar in form to the one for  $\Delta_0$ . For small  $(\Delta_a - \Delta_c)$  or when  $E_L \simeq E_0$ , the  $\frac{2}{3}$  relation between  $\Delta_1$  and  $\Delta_0$  is also satisfied for zinc-blende semiconductors. It is only when  $(\Delta_a - \Delta_c)$  is large and  $E'_0/E_L$  is significantly different from one that deviations from the  $\frac{2}{3}$  rule becomes important. A look at the band structure of zinc-blende semiconductors shows<sup>13</sup> that  $E_L$  is always larger than  $E'_0$ . Equations (15) and (18) therefore predict that in general  $\Delta_1$  is smaller than  $\frac{2}{3} \Delta_0$ . The exceptions are compounds containing P, S, N, or O where the SO splitting of the anion is smaller than that of the cation. This makes  $(\Delta_a - \Delta_c)$  less than zero, and because  $E_L > E'_0$ , it makes  $\Delta_1$  larger than  $\frac{2}{3} \Delta_0$ . These trends seem to be well satisfied in zinc-blende crystals.<sup>12</sup> Values of  $\Delta_1$  obtained from the TB parameters in Tables

II and III are shown in Table VI and compared to experimental data.

#### IV. VARIATION OF $\Delta_0$ IN SUBSTITUTIONAL ALLOYS

The simplest method of treating an alloy system is the virtual-crystal approximation (VCA), in which the alloy is assumed to be ordered, and compositionally averaged potentials or matrix elements are used. Calculations based on a straightforward application of the VCA generally show a nearly linear<sup>7,28,29</sup> dependence of SO splittings and band gaps on composition. In some cases, the arbitrariness in the choice and scaling of pseudo-potentials<sup>29</sup> for alloys or more elaborate averaging<sup>8,30-32</sup> of atomic potentials leads to nonlinear behavior.

We have used the TB method and the VCA to study the variation of  $\Delta_0$  as a function of chemical composition in  $\text{InAs}_x\text{Sb}_{1-x}$  and  $\text{In}_x\text{Ga}_{1-x}\text{As}$  alloys. In these alloys, the measured value of the SO splitting  $\Delta_0$  departs markedly<sup>1</sup> from that expected on the basis of a linear model. We find, however, that for any reasonable averaging of the TB matrix elements the VCA fails to explain the large deviations from linearity in these alloys. To separate out the effects of crystalline order from the VCA, we have done calculations for the intermediate alloys (i.e.,  $x=0.5$ ) assuming a chalcopyrite structure. In this way, although a periodic structure is used, the averaging of TB matrix elements is avoided. The use of the chalcopyrite

TABLE V. Energy levels of some zinc-blende crystals at the  $\Gamma$ ,  $X$ , and  $L$  points of the Brillouin zone obtained using the tight-binding parameters given in Table III.

Point	Level	GaP	GaAs	GaSb	InP	InAs	InSb	ZnSe
$\Gamma$	$\Gamma_{6v}$	-13.19	-12.90	-11.61	-11.16	-12.30	-11.70	-15.20
	$\Gamma_{7v}$	-0.094	-0.35	-0.79	-0.14	-0.41	-0.82	-0.42
	$\Gamma_{8v}$	0.00	0.00	0.00	0.00	0.00	0.00	0.00
	$\Gamma_{6c}$	2.88	1.52	0.86	1.42	0.36	0.25	2.90
	$\Gamma_{7c}$	5.06	4.48	3.33	4.78	4.25	3.24	7.07
	$\Gamma_{8c}$	5.20	4.72	3.69	5.09	4.65	3.78	7.20
$X$	$X_{6v}$	-9.69	-9.90	-9.40	-8.90	-10.20	-9.50	-12.50
	$X_{6v}$	-6.89	-6.90	-6.91	-5.90	-6.30	-6.41	-5.60
	$X_{6v}$	-3.78	-3.86	-3.44	-2.65	-2.82	-3.04	-2.76
	$X_{7v}$	-3.76	-3.74	-3.10	-2.58	-2.75	-2.75	-2.55
	$X_{6c}$	5.46	4.89	3.66	4.95	4.04	3.84	6.39
	$X_{7c}$	5.93	5.06	5.19	5.04	4.90	3.91	6.43
$L$	$L_{6v}$	-10.91	-10.91	-10.16	-9.66	-10.88	-10.23	-13.34
	$L_{6v}$	-6.62	-6.67	-6.51	-5.47	-5.86	-5.94	-5.24
	$L_{6v}$	-1.89	-2.03	-1.96	-1.35	-1.57	-1.81	-1.45
	$L_{4,5v}$	-1.82	-1.81	-1.49	-1.24	-1.29	-1.30	-1.20
	$L_{6c}$	3.27	2.31	2.11	2.76	1.98	1.67	3.90
	$L_{6c}$	6.93	6.36	4.88	6.13	5.68	4.70	8.29
	$L_{6c}$	7.02	6.53	5.18	6.33	5.95	5.08	8.40
	$L_{4,5c}$	7.02	6.53	5.18	6.33	5.95	5.08	8.40

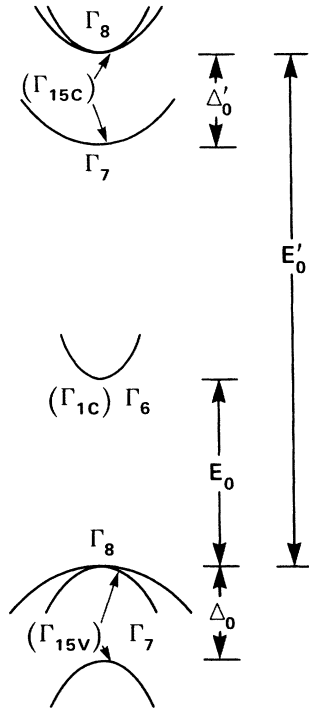


FIG. 1. Valence and conduction energy levels at  $\Gamma$  for zinc-blende crystals. The single group notation is given in parentheses.

structure gives rise to a small ( $\sim 0.01$  eV) crystal-field splitting of the states corresponding to the  $\Gamma_8$  valence states in zinc-blende crystals (when all nearest-neighbor distances are taken equal to each other). This splitting is negligible compared to  $\Delta_0$  in the alloys studied. The splitting equivalent to  $\Delta_0$  was found to be within a few hundredths of an

TABLE VI. Calculated and experimental (in parentheses) values of the spin-orbit splittings  $\Delta_0$  and  $\Delta_1$  in some diamond and zinc-blende semiconductors. The experimental data from Refs. 11 and 28 and from values listed in Ref. 24.

	$\Delta_0$	$\Delta_1$
Si	0.044 (0.044) <sup>a</sup>	0.029
Ge	0.29 (0.29) <sup>a</sup>	0.20 (0.20) <sup>a,b</sup>
$\alpha$ -Sn	0.80 (0.77) <sup>a</sup>	0.55 (0.48) <sup>a,b</sup>
GaP	0.094 (0.10, <sup>a</sup> 0.12 <sup>c</sup> )	0.07 (0.10) <sup>a,c</sup>
GaAs	0.35 (0.34) <sup>a,c</sup>	0.22 (0.23, <sup>a,b</sup> 0.22 <sup>c</sup> )
GaSb	0.79 (0.80) <sup>a,c</sup>	0.47 (0.46, <sup>a</sup> 0.47 <sup>c</sup> )
InP	0.14 (0.11, <sup>a</sup> 0.16 <sup>c</sup> )	0.10 (0.15, <sup>a</sup> 0.14, <sup>b</sup> 0.10 <sup>c</sup> )
InAs	0.41 (0.43, <sup>a</sup> 0.39 <sup>c</sup> )	0.28 (0.28, <sup>a,c</sup> 0.27 <sup>b</sup> )
InSb	0.82 (0.82, <sup>a</sup> 0.81 <sup>c</sup> )	0.52 (0.50) <sup>a,b,c</sup>
ZnSe	0.42 (0.45) <sup>b</sup>	0.25 (0.3) <sup>b</sup>

<sup>a</sup> See Reference 12.

<sup>b</sup> From experimental data given in Reference 13.

<sup>c</sup> See Reference 1.

eV from the value expected from a linear extrapolation. When the position of atoms such as In in  $\text{InAs}_{0.5}\text{Sb}_{0.5}$  was changed so that the In-As nearest-neighbor distance was different from that for In-Sb, the crystal-field splitting became larger, but  $\Delta_0$  did not decrease. To explain these results, it is interesting to look at the  $\vec{k}=0$  states in a chalcopyrite structure. These states are similar in character and "originate" from the states at the  $\Gamma$  and  $X$  points of the zinc-blende Brillouin zone. The states arising from  $X$  have a mixed  $s$ - $p$  character; the states originating from  $\Gamma$  are pure  $s$  or  $p$  in character. The ideal chalcopyrite structure does not allow the admixture of  $s$  states into the  $p$ -like  $\Gamma_{15}$ -type states. The remaining differences in the  $p$ -state energies and matrix elements between InAs and InSb (or in other alloys) are not sufficiently large to produce a nonlinear variation of  $\Delta_0$  with alloying. This seems to indicate that the observed deviations from linearity are induced by compositional disorder.<sup>7</sup> The effect of disorder is to mix  $p$  states at the top of the valence band with  $s$  states in the valence and conduction bands.<sup>7</sup> As shown below, this provides a satisfactory explanation for the bowing of  $\Delta_0$ .

In the TB picture we use, it is primarily the fluctuations in the nearest-neighbor interactions that determine the degree of  $s$ - $p$  mixing for states at the top of the valence band. The parameters  $V_{s_1p_2}(V_{s_2p_1})$  in Table III describe the interaction of a cation (anion)  $p$  state with an anion (cation)  $s$  state. For a substitutional alloy  $AB_xC_{1-x}$  the differences in the nearest-neighbor  $s$ - $p$  interaction parameters of  $AB$  and  $AC$  determine, in second-order perturbation, the degree of  $s$ - $p$  mixing. To estimate the extent of this mixing, we will make use of a "local" approximation, i.e., we assume that the  $s$ - $p$  mixing around each atom in the alloy  $AB_xC_{1-x}$  is determined by its nearest-neighbor configuration. We also assume there are no cation-cation or anion-anion bonds so that atoms  $B$  or  $C$  are always bonded to four  $A$  atoms. The five different kinds of configurations around an  $A$  atom will be denoted by  $b_n$ ,  $n=0, 1, \dots, 4$ , where  $n$  is the number of  $B$  atoms around  $A$ . The probability  $p(n)$  for the occurrence of  $b_n$  is

$$p(n) = t_n x^n (1-x)^{4-n}, \quad n=0, \dots, 4, \quad (20)$$

where  $t_0 = t_4 = 1$ ,  $t_1 = t_3 = 4$ , and  $t_2 = 6$ . If we associate a SO splitting

$$\Delta_n = \frac{1}{4}[n\Delta_{AB} + (4-n)\Delta_{AC}], \quad n=0, \dots, 4 \quad (21)$$

with each configuration, where  $\Delta_{AB}$  and  $\Delta_{AC}$  are the SO splitting  $\Delta_0$  of  $AB$  and  $AC$ , then the average value of  $\Delta_0$  defined by

$$\bar{\Delta}_0 = \sum_{n=0}^4 p(n) \Delta_n \quad (22)$$

is simply  $x\Delta_{AB} + (1-x)\Delta_{AC}$ , as can be easily verified by substituting Eqs. (20) and (21) in Eq. (22). We now discuss the effect of  $s$ - $p$  mixing on  $\Delta_n$ .

In the Slater-Koster model<sup>9</sup> the interaction of an  $s$  state at the origin with a  $p_x$  state at  $\vec{r}$  is equal to  $l_x V_{sp\sigma}$ , where  $l_x = \tau_x / |\vec{r}|$ . In the notation used here and in Ref. 10, this product is simply equal to  $\pm \frac{1}{4} V_{sp}$  when the atomic sites are the same as those in a zinc-blende structure. Since the sum of  $l_x$  over the four nearest neighbors is zero, there is no mixing of  $s$  and  $p$  states at the top of the valence bands when all four nearest neighbors of an atom are identical. When the nearest neighbors are not identical, the appropriate perturbation potential for the interaction of a bonding  $p$  state with an antibonding  $s$  state is<sup>33</sup>

$$\delta V = \frac{1}{4}(V_{s_1 p_2} - V_{s_2 p_1})_{AB} - \frac{1}{4}(V_{s_1 p_2} - V_{s_2 p_1})_{AC}. \quad (23)$$

The change in  $\Delta_n$  [Eq. (21)] caused by  $\delta V$  is of the form

$$\delta \Delta_n = [-1/E_{on} + 1/(E_{on} + \Delta_n)] \alpha_n (\delta V)^2 \quad (24)$$

or

$$\delta \Delta_n = -\Delta_n / E_{on} (E_{on} + \Delta_n) \alpha_n (\delta V)^2, \quad (25)$$

where  $\alpha_0 = \alpha_4 = 0$ ,  $\alpha_1 = \alpha_3 = 1$ , and<sup>34</sup>  $\alpha_2 = \frac{2}{3}$ . For each tetrahedral cluster we approximate  $E_{on}$  by an expression similar to that for  $\Delta_n$ , i.e.,

$$E_{on} = \frac{1}{4}[n(E_0)_{AB} + (4-n)(E_0)_{AC}], \quad n = 1, \dots, 4. \quad (26)$$

The effect of ionicity is to reduce  $\delta \Delta_n$  by the factor  $(1 - f_i^2)$ , where  $f_i$  is the Phillips<sup>26</sup>-Van Vechten<sup>27</sup> ionicity parameter.

The new values of  $\Delta_n$  determined in this way when substituted in Eq. (22) give the SO splitting for  $AB_x C_{1-x}$ . In Fig. 2 we show the calculated and measured<sup>1</sup> variations of  $\Delta_0$  with composition in  $\text{InAs}_x \text{Sb}_{1-x}$  and  $\text{Ga}_x \text{In}_{1-x} \text{As}$ . For  $\text{InAs}_x \text{Sb}_{1-x}$  and

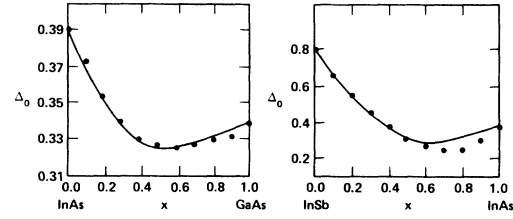


FIG. 2. Calculated variation of  $\Delta_0$  (solid line) in  $\text{In}_{1-x}\text{Ga}_x\text{As}$  and  $\text{InSb}_{1-x}\text{As}_x$  as compared to the experimental data (dots) of Ref. 1.

$\text{Ga}_x \text{In}_{1-x} \text{As}$  the parameter  $\delta V$  obtained from the  $s$ - $p$  interaction parameters listed in Table III were reduced by 14% and 18%, respectively, to improve the fit to the experimental data. The  $x$  dependence of  $\Delta_0$  obtained here particularly for  $\text{Ga}_x \text{In}_{1-x} \text{As}$  is in good agreement with experiment. The calculated results for  $\text{GaAs}_x \text{P}_{1-x}$  show a nearly linear variation of  $\Delta_0$  with  $x$ , in agreement with experimental data. For  $\text{InAs-P}$  and  $\text{Ga-InP}$ , the results are also found to be in satisfactory agreement with experiment. These results show that the disorder-induced interaction of the  $\Gamma_{15V}$  and  $\Gamma_{1C}$  (see Fig. 1) states can explain the nonlinear variation of  $\Delta_0$  in substitutional alloys.

## V. CONCLUSION

We have obtained the tight-binding interaction parameters for a number of diamond and zinc-blende crystals. Spin-orbit interactions were included in the calculations. The relation between the spin-orbit splitting of the valence bands at the  $\Gamma$  and  $L$  points of the Brillouin zone to atomic spin-orbit splittings and optical gaps was derived. The tight-binding model was used to study the variation (as a function of chemical composition) of the spin-orbit splitting at  $\Gamma$  in a number of alloy systems. It was shown that the nonlinear variation of  $\Delta_0$  is a disorder-induced effect and the bowing was related to the difference in  $s$ - $p$  interaction parameters of the alloy constituents.

<sup>1</sup>O. Berolo and J. C. Woolley, in *Proceedings of the Eleventh International Conference on the Physics of Semiconductors* (PWN Polish Scientific, Warsaw, 1972), p. 1420.

<sup>2</sup>S. S. Vishnubhatla, B. Eyglunet, and J. C. Woolley, *Can. J. Phys.* **47**, 1661 (1969).

<sup>3</sup>E. W. Williams and V. Rehn, *Phys. Rev.* **172**, 789 (1968).

<sup>4</sup>A. G. Thompson *et al.*, *Phys. Rev.* **146**, 601 (1966).

<sup>5</sup>A. Ebina *et al.*, *Phys. Rev. B* **6**, 3786 (1972).

<sup>6</sup>C. Alibert *et al.*, *Phys. Rev. B* **6**, 1301 (1972).

<sup>7</sup>J. A. Van Vechten, E. Berolo, and J. C. Woolley, *Phys. Rev. Lett.* **29**, 1400 (1972).

<sup>8</sup>R. Hill, *J. Phys. C* **7**, 516 (1974).

<sup>9</sup>J. C. Slater and G. F. Koster, *Phys. Rev.* **94**, 1498 (1954).

<sup>10</sup>D. J. Chadi and M. L. Cohen, *Phys. Status Solidi B* **68**, 405 (1975).

<sup>11</sup>M. Cardona and D. L. Greenaway, *Phys. Rev.* **125**, 1291 (1962).

<sup>12</sup>M. Cardona, K. L. Shaklee, and F. H. Pollak, *Phys. Rev.* **154**, 696 (1967).

<sup>13</sup>J. R. Chelikowsky and M. L. Cohen, *Phys. Rev. B* **14**, 556 (1976), and references therein.

<sup>14</sup>R. Pollak *et al.*, *Phys. Rev. Lett.* **29**, 1103 (1973);

- L. Ley *et al.*, Phys. Rev. B 9, 600 (1974).
- <sup>15</sup>W. D. Grobman and D. E. Eastman, Phys. Rev. Lett. 29, 1508 (1972); D. E. Eastman, *et al.*, Phys. Rev. B 9, 3473 (1974).
- <sup>16</sup>E. O. Kane, Phys. Rev. B 13, 3478 (1976).
- <sup>17</sup>J. C. Phillips, Rev. Mod. Phys. 42, 317 (1970); in particular, see discussion in Appendix, p. 354.
- <sup>18</sup>J. C. Phillips and L. Liu, Phys. Rev. Lett. 8, 94 (1962).
- <sup>19</sup>It has been pointed out by Phillips and Liu (Refs. 17 and 18) that in the tight-binding picture the renormalization tends to reduce (increase) the valence (conduction) band spin-orbit splitting. Experimentally the reverse is found to be true. The problem arises from restricting the basis set to *s* and *p* functions only.
- <sup>20</sup>R. J. Elliot, Phys. Rev. 96, 266 (1954).
- <sup>21</sup>R. Braunstein and E. O. Kane, J. Phys. Chem. Solids 23, 1423 (1962).
- <sup>22</sup>R. Braunstein, J. Phys. Chem. Solids 8, 280 (1959).
- <sup>23</sup>J. C. Phillips, *Bonds and Bands in Semiconductors* (Academic, New York, 1973).
- <sup>24</sup>F. Herman *et al.*, Phys. Rev. Lett. 11, 541 (1963).
- <sup>25</sup>E. Clementi and C. Roetti, At. Data Nucl. Data Tables 14, 177 (1974).
- <sup>26</sup>See Ref. 17.
- <sup>27</sup>J. A. Van Vechten, Phys. Rev. 182, 891 (1969).
- <sup>28</sup>D. J. Chadi and M. L. Cohen, Phys. Rev. B 7, 692 (1973).
- <sup>29</sup>J. A. Van Vechten and T. K. Bergstresser, Phys. Rev. B 1, 3351 (1970).
- <sup>30</sup>D. Jones and A. H. Lettington, Solid State Commun. 7, 1319 (1969).
- <sup>31</sup>D. Richardson, J. Phys. C 4, L289 (1971), and 5, L27 (1972).
- <sup>32</sup>R. Hill, J. Phys. C 7, 521 (1974).
- <sup>33</sup>For the interaction with a bonding *s* state the perturbation potential would be the difference in the average *s-p* interactions of the alloy constituents.
- <sup>34</sup>For  $n=2$  the interaction of a bonding *p* state with an antibonding *s* state gives 0,  $2\delta V$  or  $-2\delta V$  with equal probability. The average of the squares is  $\frac{8}{3}(\delta V)^2$ .